

Tasks Unlimited: Lightweight Task Offloading Exploiting MPI Wait Times for Parallel Adaptive Mesh Refinement

Philipp Samfass^{*1}, Tobias Weinzierl², Dominic E. Charrier², and
Michael Bader¹

¹Department of Informatics, Technical University of Munich,
Garching, Germany

²Computer Science, Durham University, Durham, Great Britain

September 16, 2019

Abstract

Balancing dynamically adaptive mesh refinement (AMR) codes is inherently difficult, since codes have to balance both computational workload and memory footprint over meshes that can change any time, while modern supercomputers and their interconnects start to exhibit fluctuating performance. We propose a novel lightweight scheme for MPI+X which complements traditional balancing. It is a reactive diffusion approach which uses online measurements of MPI idle time to migrate tasks from overloaded to underemployed ranks. Tasks are deployed to ranks which otherwise would wait, processed with high priority, and made available to the overloaded ranks again. They are temporarily migrated. Our approach hijacks idle time to do meaningful work and is totally non-blocking, asynchronous and distributed without a global data view. Tests with a seismic simulation code running an explicit high order ADER-DG scheme (developed in the ExaHyPE engine, www.exahype.org) uncover the method’s potential. We found speed-ups of up to 2–3 for ill-balanced scenarios without logical modifications of the code base.

1 Introduction

Load balancing that decomposes work prior to a certain compute phase—a time step or iteration of an equation system solver—is doomed to underperform in many sophisticated simulation codes. There are multiple reasons for this:

^{*}samfass@in.tum.de

The clock frequency of processors changes over runtime [9, 2, 8], the network speed is subject to noise due to other applications [20, 27] or IO, and task-based multicore parallelisation (MPI+X) tends to yield fluttering throughput due to effects of the memory hierarchy [24], work stealing and non-determinism in the MPI progression. While this list is not comprehensive, notably modern numerics drive the non-predictability: They build atop of dynamic adaptive mesh refinement (AMR) that changes the mesh throughout a time step or mesh sweep, combine different physical models, or solve non-linear equation systems with iterative solvers in substeps. It becomes hard or even impossible to predict a step’s computational load. As adjusting parallel partitions and respective data migration is often costly, many AMR codes consequently repartition only every 10th or 100th time step and tolerate certain load imbalances.

We propose a novel, lightweight load redistribution scheme that acts on top of traditional load balancing. It assumes that parts of the underlying simulation code are phrased in terms of tasks. Our idea is to offload tasks from overbooked to waiting ranks to make these work productively rather than being idle. The code plugs into the MPI operations searching for the late sender pattern [23], which yields a wait graph. Ranks identify that they are critical to the walltime, search for “optimal victims”, i.e. ranks that can take up further work without slowing down the overall computation, and then actively offload tasks to victim ranks. We assume that neither load distribution nor imbalances change radically in-between algorithm steps. We therefore update the wait graph on-the-fly, using concepts from reinforcement learning [5], and let the wait graph guide a diffusion of tasks to follow load alterations. To our knowledge, this is the first approach that abandons the attempt to perfectly balance work in a predictive way but rather explicitly determines and hijacks MPI wait times to guide a lightweight task distribution.

Task-based parallelisation between MPI ranks is not new. The UIntah framework [12, 25] for example uses a centralised data/task warehouse from which ranks are served. Tasks therefore are not tied to a particular rank and the ownership is (logically) with the warehouse. The Swift project [31] as another example phrases a whole SPH simulation in terms of tasks and applies graph partitioning to derive task decomposition and task migration patterns over the whole machine, i.e. both shared and distributed memory domains. This is a wholistic, fine-granular, proactive load balancing approach. Charm++ [1] features tasks that can be migrated and a runtime which tracks task dependencies in-between ranks dynamically. Dependencies thus pose no constraint on the task placement. Other task-based approaches such as HPX [21, 33] feature task migration between different processes via a global address space. The AMR framework sam(oa)² finally demonstrates a reactive task stealing approach that is entirely driven by the application [30] in-between bulk-synchronous processing. While our approach takes up ideas and extends upon existing work, it differs in the following fundamental ways: (i) It does not target load distribution per se but determines MPI waiting times to improve upon existing load balancing. It is a reactive rather than a predictive add-on to load balancing. (ii) It is very fine-grained as it acts on the level of individual (compute-intense) tasks. Yet, no

task dependencies are tracked. We work non-persistently. Tasks are offloaded to other ranks, processed there, and the results are immediately sent back. (iii) It is a lightweight approach since the task migration is realised through a set of tasks itself. Therefore, we plug seamlessly into the tasking system and the overhead is small. We do not need a dedicated load balancing or MPI progression thread [18]. (iv) It gives ranks the opportunity to outsource tasks. This opportunity “window” is opened reactively, i.e. ranks know how many tasks they are allowed to give away and they consequently use this for non-urgent tasks: Tasks are given away proactively, i.e. prior to one rank running idle. We bring together the best of two worlds: proactive task outsourcing and the reaction to runtime changes. This strategy differs from the aforementioned approaches.

Its properties render our approach promising for many applications which are already phrased in tasks. We assess it by means of an earthquake simulation benchmark. The underlying code base ExaHyPE [4, 28] relies on an explicit time stepping scheme, which works on dynamically adaptive meshes. The setup poses a challenge to our approach as it is not dominated by few compute-intense tasks. We benchmark the reactive scheme against sole geometric domain decomposition and against a task distribution which is derived from chains-on-chains partitioning (CCP) [26].

Our manuscript is organised as follows: We introduce the benchmark code in Sect. 2 before we phrase our vision (Sect. 3). Some terminology (Sect. 4) allows us to introduce a set of load balancing strategies in Sect. 5. This core contribution starts from a point-to-point diffusion approach which is augmented and accelerated by various techniques. In Sect. 6, we elaborate on the technical details of our implementation. Some experiments in Sect. 7 highlight the potential of the approach. We close the discussion with an interpretation of the scheme’s characteristics (Sect. 8), before we identify further application areas of the proposed methodology plus future work in Sect. 9.

2 A parallel ADER-DG seismic solver on adaptive meshes

Our benchmark code implements an explicit high order discontinuous Galerkin solver for the linear elastic wave equations, which may be written as (cf. [19], e.g.)

$$\begin{aligned} \frac{\delta \sigma}{\delta t} - E(\lambda, \mu) \cdot \nabla v &= S_\sigma, \\ \frac{\delta v}{\delta t} - \frac{1}{\rho} \nabla \cdot \sigma &= S_v, \end{aligned}$$

with a velocity field v and a stress tensor σ in the first equation of the system. It results from Hooke’s law and evolves both quantities through a stiffness tensor E depending on the Lamé constants λ and μ (i.e., material parameters). The second equation describes Newton’s second law. ρ here is the density of the material.

As simulation setup, we use the established Layer Over Halfspace 1 (LOH.1) benchmark [13]. It mimics an earthquake via a simplified setting that assumes a point source in a cubic domain that consists of two material layers: a thin sediment layer (with slower wave speeds) over a rock layer (with higher wave speeds). LOH.1 is part of a widely-used collection of benchmark scenarios to validate codes and compare results with other simulation software.

ADER-DG: High Order Discontinuous Galerkin

Our solver realises an Arbitrary high-order DERivative discontinuous Galerkin (ADER-DG) method [36] on tree-structure Cartesian grids. It is implemented within the ExaHyPE engine to solve hyperbolic PDE systems [28]. In the following, we summarize the main computational steps of the scheme, whereas we describe full details of the scheme in [11].

ADER-DG is an explicit time-stepping scheme that decomposes each time step into three phases, thus computing $(\sigma, v)(t + \Delta T) = (\mathcal{C} \circ \mathcal{R} \circ \mathcal{P})(\sigma, v)(t)$. Each grid cell approximates the solution locally via a tensor product of polynomials of degree p (orthogonal polynomials constructed on Gauss-Legendre points), following a classical DG-SEM (DG Spectral Element Method) approach [17]. In the *predictor* step \mathcal{P} , the algorithm first extrapolates the solution in time, ignoring the influence of neighbouring cells and evolves (σ, v) . This step follows the Cauchy-Kovalevskaya procedure [15]. The arising discontinuities in the predicted solution (σ, v) along the cell faces are next subject to a space-time Riemann solver \mathcal{R} . Finally, we bring the Riemann solution and the predicted value together, i.e., correct (\mathcal{C}) the predicted value.

Our code discretises our computational domain through a spacetime [34] and thus solves the problem on an adaptive Cartesian grid where the individual cells are cubes. Each cell may be transformed according to a curvi-linear transformation (as in [17]) to align to geometry features: Each cell carries a transformation matrix which fits it to the actual topology, allowing simulation of seismic wave propagation in complex topographies. For the LOH.1 benchmark, the transformation matrix is simple (but causes the same computational load), as it only aligns the material discontinuity in the LOH.1 geometry to our Cartesian grid. We adaptively refine the mesh in the top sediment layer and around the point source. We coarsen towards the other boundaries to reduce reflections due to non-perfectly absorbing boundary conditions.

Parallel Implementation of ADER-DG

Per time step, the $\mathcal{C} \circ \mathcal{R} \circ \mathcal{P}$ sequence of cell/face/cell operations is applied to the adaptive grid which is geometrically partitioned. We use a non-overlapping domain decomposition where the Riemann tasks along the domain boundaries are computed redundantly by each adjacent rank.

The three ADER-DG phases translate into three types of tasks. Prediction tasks correspond to cells, Riemann tasks to faces, and correction tasks again to cells. Out of the three task types, the predictions \mathcal{P} are the computationally

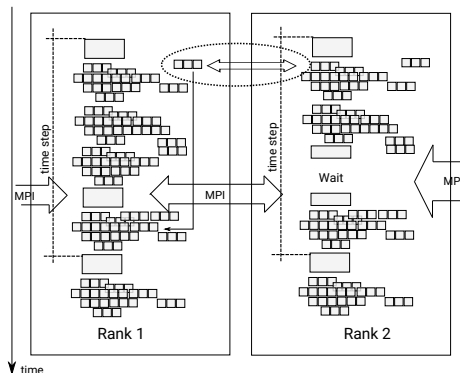


Figure 1: Schematic program execution: Ranks decompose into tasks. Some tasks’ outcomes are required only late throughout the computation or even after the boundary data exchange or in the next time step. High bandwidth demands arise towards the end of the time step, i.e., we are not consistently bandwidth-bound. Our scheme offloads non-urgent tasks to MPI ranks that tend to wait and immediately transfer the outcome back (tasks within the dotted circle belong to rank 1 but are computed on rank 2). The remote completion is almost hidden from the local rank’s workflow.

dominant ones. They make up more than 97% of the runtime for our experiments with polynomial order $p = 7$. $p = 7$ is the order we observed the best time-to-solution per accuracy for our experiments. While they are expensive, they work per cell, i.e., have well-defined memory needs, and they are totally independent of each other. Nevertheless, they decompose into two categories [10] of \mathcal{P} tasks. One category are tasks/cells whose faces are adjacent to a resolution transition—that is, neighbouring cells have a different resolution—or cells which are adjacent to a domain decomposition boundary. The other category of \mathcal{P} tasks is formed by all the remaining \mathcal{P} s. Each \mathcal{P} task feeds its output into $2d$ Riemann tasks \mathcal{R} . Obviously, a Riemann task \mathcal{R} however might depend on more than two prediction tasks if it corresponds to a face along a resolution transition. If an \mathcal{R} task corresponds to a face along the MPI boundary, it furthermore requires input data running through the network. Our first category of prediction tasks—the same applies to corrections—all have dependencies with such “sophisticated” Riemann tasks. All Riemann tasks are computationally lightweight. After completion of all $2d$ Riemann solves which surround one cell, the time step’s final correction task \mathcal{C} is triggered. \mathcal{C} is comparably cheap, too.

As we work with a task-based formalism, our code can work with fully non-blocking boundary data exchange. Upon the completion of a prediction job which is adjacent to a partition boundary, we send out the output immediately. As our steps are phrased in tasks, we then continue with further prediction tasks or postpone Riemann tasks which are not ready yet due to missing incoming data. This yields a classic MPI+X parallelisation where the boundary

exchanges do not synchronise the individual ranks (Fig.1). Our (baseline) code is neither bandwidth-bound all the time nor consists of distinguishable different phases. The task formalism intermixes the three compute steps \mathcal{C} , \mathcal{R} , \mathcal{P} [10] and this melange of different activities is interwoven with MPI data transfer in the background [10]. If bandwidth restrictions arise, they arise as bursts towards the end of each time step. The code is MPI bandwidth-demanding yet not bandwidth-bound always.

Optimistic time stepping with weakened temporal and spatial constraints

Explicit time stepping for hyperbolic equations suffers from strong synchronisation: The outcome of one time step has to be globally reduced, as we have to determine the admissible time step size from the CFL condition, and this admissible time step size then feeds into the ranks again. This is an allreduce.

For the present application scenario, a dynamic time step adaption is over-engineered. As long as the PDE remains linear and no boundary conditions such as dynamic rupture are imposed which dramatically change the temporal scale of the studied phenomena, the admissible time step size remains invariant. To future-proof the code, we nevertheless realise the global CFL data exchange.

Once we assume that time step size is known or that our code can reliably estimate the evolution of the admissible time step size a priori, we can eliminate the strict global synchronisation of the ranks. While a rank waits for an exchange of global information, incoming Riemann data or AMR information, it can already process \mathcal{P} tasks of the subsequent time step. Performance analysis thus has to be done carefully: While a rank waits to complete its time step, and, hence, cannot logically kick off the next time step, it might still have work to do which logically belongs into this very next time step. Our methodology amplifies this effect.

The \mathcal{R} and \mathcal{C} tasks have to run close to the memory. They are cheap and notoriously memory- or latency-bound. \mathcal{P} tasks in contrast are candidates to be deployed to remote compute devices: they cause the primary computational load and they are typically not immediately time-critical, at least not in the moment they are spawned. Other predictions are in the task queue, and there is a high probability that further Riemann and correction steps of the previous time step still have to be processed. We therefore call prediction tasks *offloadable*.

3 Methodological vision

We assume that the work in our code is already reasonably distributed via a distribution of data (grid cells, etc.) to MPI ranks. We however accept that even sophisticated dynamic AMR codes will fail to achieve perfect balancing of computing times. This can be due to variable computational load per data entity (grid cell) in complicated models and numerical schemes but also due to the complex hardware and performance behaviour of modern machines. An

additional motivation can be to proceed with a non-perfect load distribution, because of high data-redistribution costs.

In MPI+X codes, imbalance eventually manifests in MPI waits. We therefore determine approximate waiting times—the measured “wait” is reduced by the time a rank could spend on dangling tasks that are not critical for progress—and build a wait graph that allows us to determine bottleneck ranks. However, it is too late to react once ranks become idle, as we would essentially create further waiting times to move around tasks. Instead, we implement proactive task offloading in the sense that a *critical rank* (identified as being too slow) will offload tasks to under-employed *victim ranks* ahead of time (i.e., *proactively*) and based on knowledge from previous time steps. Hence, our reactive task offloading teams up with traditional data decomposition and migration, and helps to improve load balancing. It finally is hidden away from the code, i.e., it is a lightweight extension.

We further exploit that our AMR code contains strongly compute-bound kernels. Hence, despite bandwidth access peaks caused by memory-bound kernels, we have bandwidth available in-between these peaks. *We propose to hijack MPI wait times and available bandwidth on “too fast” ranks to process tasks that are “stolen” from “too slow” ranks:* We take compute-intense jobs from ranks that delay other ranks and process them on ranks which wait for other ranks. This works as we process such tasks with high priority on the idle ranks, and thus send tasks forth and back at times when the ranks are not suffering from bandwidth constraints. The result is a reactive load balancing approach which is orthogonal to, i.e., works on top of classic load balancing.

4 Terminology

Our algorithm is constructed around simple terminology and a few definitions. Let $N^{(\text{ranks})}$ denote the number of MPI ranks. $0 \leq i, j < N^{(\text{ranks})}$ always holds for indices i, j . Each rank employs $N^{(\text{cores})}$ cores. They realise the time stepping algorithm, i.e., process $\mathcal{C}, \mathcal{R}, \mathcal{P}$. They notably also process all remote \mathcal{P} tasks, i.e., tasks sent in by another rank, processed locally, but then sent back. We denote $N_i^{(\text{tasks})}(t)$ to be the number of these tasks at a certain time t on rank i . As tasks are migrated, spawned throughout the time step, and completed, $N_i^{(\text{tasks})}(t)$ changes all the time. Finally let $t^{(\text{task})}$ be the time one core requires to complete one of the offloadable tasks. We assume they are atomic, i.e., run exclusively on one core at a time. $t^{(\text{task})}$ quantifies the cost of \mathcal{P} . Sampling determines it.

Per time step, our code exchanges boundary data with neighbouring ranks as well as a global time step size.

Our reactive load balancing plugs into these data exchanges. We found it sufficient to track the global exchange only, but the concept could be applied to the boundary exchange, too. It thus holds also in the absence of global synchronisation.

Definition 1. Our code runs into situations where a rank i (logically) stops and can not continue until a message from rank j arrives. Let the **waiting time** $t_{i,j}^{(wait)}$ be the core time that elapses in-between.

In a BSP-type environment (bulk synchronous processing) where a rank forks threads, joins these again, and then finishes all data exchange, $t_{i,j}^{(wait)}$ is a simple online measurement quantity:

$t_{i,j}^{(wait)} = N^{(cores)}(T_{i,j}^{(start)} - T_{i,j}^{(end)})$, where $T_{i,j}^{(start)}$ is the time stamp when rank i receives the kick-off message of the subsequent time step from rank j and $T_{i,j}^{(end)}$ is the time stamp when data exchange between i and j ends (these are typically sends). $t_{i,j}^{(wait)}$ sums up all core wait times (which are equal) and thus scales with $N^{(cores)}$.

In an asynchronous task environment tasks of a time step n that are not critical to the progress of the rank may overlap with computations of time step $n + 1$. We therefore reduce the wait time $t_{i,j}^{(wait)}$ by an additional term:

$$t_{i,j}^{(wait)} = \max\left(0, N^{(cores)}(T_{i,j}^{(start)} - T_{i,j}^{(end)}) - N_i^{(tasks)}t^{(task)}\right). \quad (1)$$

$N_i^{(tasks)}t^{(task)}$ quantifies how much of the wait time can be spent productively on handling ready tasks. It is a crude estimate as $N_i^{(tasks)}$ might change dramatically throughout this time. Consequently, we use the max function to avoid negative wait times.

Definition 2. Rank i is called a **critical rank** if $\forall j : t_{i,j}^{(wait)} = 0$ and $\exists j : t_{j,i}^{(wait)} > 0$.

A critical rank is a rank that does not wait for any other rank but delays at least another one.

While there may be more than one critical rank, we usually identify the most critical one to offload task from it to underloaded victim ranks:

Definition 3. Let $t_{max}^{(wait)} = \max_{i,j} t_{i,j}^{(wait)}$. A rank i is an **optimal victim** if $\nexists j : t_{j,i}^{(wait)} > 0$ and $\exists j : t_{i,j}^{(wait)} = t_{max}^{(wait)}$.

An optimal victim is the rank in the system that could take up the biggest chunk of further work without decreasing the performance, since it idles the longest. Our goal is to make critical ranks deploy more and more tasks to optimal victims until they cease to be critical. For this, we introduce a quantity $N_{i,j}^{(offload)}$ per rank which clarifies how many tasks from rank i should be deployed to rank j . Rank i then plugs into the task spawn mechanism. We outsource the first $N_{i,j}^{(offload)}$ offloadable tasks that become ready throughout a time step to rank j . In a task-based environment the “first” is to be read weakly, as the runtime might reorder them.

As we work in a distributed environment with changing meshes, non-constant numeric cost, and hardware noise, this type of non-persistent load balancing can fail:

Definition 4. An *emergency* arises for rank j if $\exists i : N_{i,j}^{(\text{offload})} > 0$ and $t_{i,j}^{(\text{wait})} > 0$.

Emergency means that a rank both deploys data to a victim rank and is delayed by this very rank. This may happen when the victim rank is overloaded, if we suffer from network congestion or if too many messages (remote tasks) stress the MPI subsystem such that results are not sent back fast enough to the deploying rank. As soon as we spot such an emergency, we add a rank to a black list.

Definition 5. The *blacklist* is the set of ranks that may not take up more work. We hold one blacklist per rank.

Our terminology circumscribes a greedy graph optimisation algorithm. We establish a *wait graph* over all ranks. $t_{i,j}^{(\text{wait})}$ serves as edge weight in this directed graph. If we mask out zero weights, the graph is sparse. The critical rank is the last rank along a critical path through the set of ranks. The “last” edge points to the critical rank. Multiple critical ranks may exist. Our goal is to remove the head from the critical path and then to continue iteratively.

To achieve this goal, we label those ranks in the graph which are origins of wait paths with the biggest wait time as optimal victims. They can take up further work without slowing down the overall computation. The determined numbers of task offloads $N_{i,j}^{(\text{offload})}$ establish a *task distribution graph* on top of our rank vertices. It connects sinks of the wait graph with sources of critical paths.

5 Lightweight load balancing

Once the MPI wait times are identified, each rank i maintains statistics of $N_i^{(\text{tasks})}(t)$. It measures all $t_{i,j}^{(\text{wait})}$ and it samples execution times to determine $t^{(\text{task})}$. Furthermore each rank has a blacklist of ranks that return remote tasks too slowly. All statistics are sampled over time spans through

$$\tilde{x} = \frac{\sum_{l=0}^S (\omega^{(\text{avg})})^l x_l}{\sum_{l=0}^S (\omega^{(\text{avg})})^l}, \quad \text{with a fixed } \omega^{(\text{avg})} \in]0, 1]. \quad (2)$$

x_0, \dots, x_S are the measurements from the $S + 1$ most recent time steps (x being a placeholder for our quantities of interest). We drop older measurements as further quantities alter the moving average by less than 10% for $\omega^{(\text{avg})} \approx 0.9$.

Our global statistics allow us to introduce various algorithms to determine $N_{i,j}^{(\text{offload})}$, i.e., how many tasks each rank i has to deploy to rank j . We update $N_{i,j}^{(\text{offload})}$ prior to each time step with the most recent statistics at hand. From hereon, newly spawned offloadable tasks on i can be offloaded to another rank j as long as they haven’t exceeded our quota $N_{i,j}^{(\text{offload})}$. This definition implies that we never delegate stolen tasks further, i.e. only tasks produced locally are “stolen” by another rank.

In order to improve parallel performance in the presence of critical ranks, we propose different strategies.

Reactive load balancing

Each rank can determine its optimal number of tasks $N_{i,j}^{(\text{opt})}$ that it has to deploy to other ranks from the global data view (Alg. 1). The iterative approach identifies the unique critical rank, computes how much it could “fill up” the optimal victim, adopts the load distribution, and then waits for the next time step’s measurements.

Algorithm 1 Blueprint of reactive load balancing.

```

function REACTIVELB(rank  $i$ )
   $\forall k \neq i$  exchange  $t^{(\text{wait})}$  (non-blocking allgather)
  Compute critical rank  $m$ 
  if  $m = i$  then
    Compute optimal victim  $n$ 
     $N_{i,n}^{(\text{opt})} \leftarrow 0.5t_{\text{max}}^{(\text{wait})}/t^{(\text{task})}$ 
  end if
end function

```

The algorithm’s use of the term optimal in $N^{(\text{opt})}$ is misleading for several reasons: First, it is a backward-looking optimum which derives an optimal task distribution for the passed time step. With AMR, the grid however might change in the present step. Second, it relies on a weak consistency model for its input quantities, as we use non-blocking allgather. Some data used in the computation thus might be outdated. Third, the quantities themselves rely on $N_i^{(\text{tasks})}(t)$ which is a snapshot of the local runtime’s state. Fourth, the formula is based upon a real-time measurement of $t^{(\text{task})}$ which we determine through a weighted averaging over multiple probes. If a core downclocks due to high energy consumptions [9] or failures, this does not immediately reflect in the timings. Finally, though our formalism sticks to unique critical workers and optimal victims, it can happen that the asynchronous balancing makes multiple ranks consider themselves to be critical.

Diffusion

There is limited sense in using $N_{i,j}^{(\text{opt})}$ as it is only a guideline which tends to rebalance aggressively. It grabs one victim rank’s MPI time completely in one rush. We therefore introduce per rank a relaxation factor $0.1 \leq \omega_i^{(\text{diff})} \leq 1$ and determine a task distribution from the optimal distribution plus the current state:

$$N_{i,j}(k+1) = \omega_i^{(\text{diff})} N_{i,j}^{(\text{opt})}(k) + (1 - \omega_i^{(\text{diff})}) N_{i,j}(k).$$

$\omega^{(\text{diff})} \approx 1$ makes the diffusion adopt the “optimal” task distribution quickly,

while a small $\omega^{(\text{diff})}$ yields a moving average. The actual distribution is incrementally fitted to the optimal distribution.

We may consider our overall optimisation problem to be strongly nonconvex and subject to fluctuations. To reduce the risk to run into local minima with small $\omega^{(\text{diff})}$, but also to reduce the risk to introduce massive distribution fluctuations, we increment $\omega^{(\text{diff})} \leftarrow \min(\omega^{(\text{diff})} + 0.1, 1)$, if

$$\forall i : \frac{\sum_j |N_{i,j}^{(\text{opt})}(k+1) - N_{i,j}^{(\text{offload})}(k)|}{\sum_j |N_{i,j}^{(\text{opt})}(k) - N_{i,j}^{(\text{offload})}(k-1)|} \geq \omega^{(\text{reinf})} \quad (3)$$

Otherwise, $\omega^{(\text{diff})} \leftarrow \max(0.9\omega^{(\text{diff})}, 0.1)$. $\omega^{(\text{reinf})} \in]0, 1]$ is fixed.

While a decrease of $\omega^{(\text{diff})}$ by 10% ensures that our diffusion updates usually become smaller and smaller, we increase the relaxation if two subsequent iterations drag the update with a certain intensity. The latter typically happens if ranks enter the blacklist:

Blacklisting

Our load balancing strategies can run into situations where they overbook ranks and thus slow down the overall computation – despite the damping of the updates through $\omega^{(\text{diff})}$. The paragraph following Definition 4 enlists reasons for this and introduces blacklists that accommodate this problem.

Whenever a victim rank does not deliver the result of a stolen task back fast enough, the origin rank identifies this emergency and adds the victim rank to its local blacklist. Blacklists are subject to our non-blocking all-gather communication and thus shared globally. The update of the local load distribution sets $N^{(\text{opt})} = 0$ for any blacklisted communication partner. In a diffusive world, this triggers a gradual retreat from overbooked ranks.

We found it valuable to use an annotated blacklist set where each entry holds a weight. As long as emergencies arise for a particular rank, its blacklist value is incremented by one. After each rebalancing round, we decrement the weight by 10%. Blacklist entries with a weight below 0.5 are eventually removed from the blacklist. We avoid oscillations: If a rank has entered the blacklist, it remains on this list for a while to avoid that it is immediately rebooked after enough tasks have been retreated.

(Reduced) Chains-on-chains partitioning

Diffusion yields a slow process. This is especially true at startup if we start from an ill-suited domain decomposition. Furthermore, no iterative technique is safe from running into local minima. It is hence reasonable to benchmark against an “optimal” task distribution that is computed for a given grid setup. The term optimal however is to be chosen carefully, as any precomputation relies on an a-priori cost model which can only approximate the actual machine behaviour. We use a uniform cost model for \mathcal{P} which neglects data transfer cost.

Chains-on-chains (CCP) partitioning [26] is one approach to determine good task distributions. It can be defined as partitioning of a 1D chain of $\sum_i N_i^{(\text{tasks})}$ tasks into $N^{(\text{ranks})}$ partitions such that the bottleneck load (maximum load assigned to a rank) is minimized. With uniform cost per task, the CCP problem reduces to a much simpler problem: we only need to “cut the chain” of tasks into $N^{(\text{ranks})}$ equally sized pieces, i.e., the bottleneck load will then be equal to the average load over all ranks (± 1 task). The number of tasks per rank is known after the initial mesh was built on every rank. We use a single collective allgather step to distribute this information among all MPI ranks. Every rank then solves the reduced CCP problem using a simple search algorithm. This results in a new unique partitioning that defines how many tasks every rank needs to give to other ranks such that the new load on every rank is rendered equal to the average load.

6 Implementation

The success of our reactive, lightweight load balancing hinges upon an efficient, low-overhead realisation. In particular, we rely on fast task migration for an irregular, a-priori unknown dynamic communication pattern. We found that prioritized task processing and full overlap of task communication are essential. The latter requires dedicated attention from a technical standpoint, as sufficient “progression” of MPI messages needs to be ensured.

Our implementation is based on Intel’s Threading Building Blocks (TBB) [29] which we extended by a custom priority mechanism: We employ as many real TBB tasks as we have cores per rank. These TBB tasks process (consume) our own, logical tasks managed through TBB’s priority queue. We found this solution to outperform the native TBB priorities.

Task lifecycle and decision making

Our runtime distinguishes three types of tasks: High priority tasks, low priority tasks and offloadable tasks. Low priority is the default. The offloading hooks into the actual creation of offloadable tasks.

The hook makes the decision whether a task is enqueued locally or can be offloaded. For this, it combines three criteria (Alg. 2): The task has to be offloadable (have reasonable high arithmetic intensity and cost), there have to be more than C tasks in the local task queue, and there has to be a victim rank. We store an atomic counter for each target rank j of i . It counts how many tasks still might be offloaded to rank j . It is updated per time step by the load balancing. If a task is given away, the respective counter is decremented. As we may need to offload tasks to multiple victim ranks, victims are selected in a round-robin fashion. Round-robin ensures that victim ranks can start to process offloaded tasks as soon as possible.

We exploit that each task is ready when it is spawned. For codes with task dependencies, the offload decision would need to hook into the transition of

Algorithm 2 Spawn process of a ready task on rank i . At the start of each time step $\hat{N}_{i,j}^{(\text{offload})} \leftarrow N_{i,j}^{(\text{offload})}$.

```

function SPAWNTASK(rank  $i$ , task  $x$ )
   $notStarved = N^{(\text{tasks})} > C$                                 ▷ Avoid rank starvation
  if  $notStarved \wedge canOffload(x)$  then
     $j = pickarg_k\{\hat{N}_{i,k} > 0\}$                                 ▷ Round robin
    if  $j \neq \perp$  then
       $\hat{N}_{i,j}^{(\text{offload})} \leftarrow \hat{N}_{i,j}^{(\text{offload})} - 1$         ▷ Atomic
      Send  $x$  to rank  $j$ 
    end if
  else
    Enqueue  $x$  with low priority
  end if
end function

```

a task into ready. Giving away tasks too aggressively can lead to starvation of rank-local task consumers. We face a classical consumer-producer challenge: The code spawns tasks only at a certain speed and puts them into the job queue. Besides the limited speed, not all tasks are offloadable. Hence, if we give away tasks too aggressively to other ranks—which act as additional consumers—the task job queue may run out of tasks for local processing. To avoid this, we only offload a task if enough tasks remain available to keep the local task consumers busy. This guarantees optimal utilization of both local and remote resources.

Tasks that are offloaded logically split up into two tasks: While the actual task is sent away and computed remotely, we logically insert a single receive task for all offloaded tasks. The runtime will poll this receive task as part of the standard task processing. Once a remote task starts to send its results back, the receive task finalises the corresponding MPI receives and cleans up all data structures. The task offloading itself is not visible to the application.

To ensure that offloaded tasks are sent back early, i.e., to ensure that we make optimal use of the network, we issue offloaded tasks with high priority. They are thus computed prior to local tasks.

Creating the reactive communication graph

Predictive load balancing algorithms, such as CCP, use a dedicated synchronization step where load balancing meta-information is exchanged. As a result, all communication partners are known prior to the actual computation and `MPI_Irecv`s can be posted at the time of the load migration. In our reactive scheme, we do not explicitly exchange meta-information, the communication pattern changes frequently and the round robin task distribution makes it impossible to predict the exact data flow as well as the number of messages to be transferred. Finally, tasks are to be sent out as soon as possible, i.e., we may not aggregate tasks.

Our algorithm resembles a one-sided data exchange model where many small tasks are “put” to another rank and have to “trickle through” while the numerical algorithm is running. Without a mutual a-priori agreement on the communication pattern and the size of receive windows, i.e., the data cardinality, we however issue one asynchronous data send per task that is to be offloaded, and we use `MPI_Iprobe` to detect tasks that are to be received.

This yields many small non-blocking data transfers. Their efficient realisation, i.e., the quick establishment of data flows—we may assume that they are large enough to prohibit eager buffering—is very important as we have to release critical ranks from work. We make an additional task realise the `MPI_Iprobe` pick ups. It polls MPI, establishes incoming data connections, i.e., launches receives, and eventually reschedules itself after all the other ready tasks. Therefore, the task’s mean time between activation automatically depends on the load: The longer the task queue the longer it will take until the probing is executed again. In phases of high computational load, CPU time is mostly dedicated to computation. In phases of low computational load, in particular whenever a rank is underloaded and thus a potential victim, rescheduling ensure that tasks are received quickly. We busy-poll MPI. Once a remote task completes, its host rank, i.e., the victim, triggers a send back. It is another non-blocking send which is eventually picked up by the probes on the task’s origin.

MPI progression

Our code stores all pending sends and receives, i.e., the `MPI_Request` handles, in a central broker (“request manager”). They are held FIFO. A central difficulty with many non-blocking MPI messages and a dynamic exchange pattern, however, is progressing messages in the background. Issuing solely `MPI_Isend` does not ensure that the actual message transfer occurs fully in the background without any further CPU involvement [18]. We cannot be sure that MPI makes sufficient progress.

One possible remedy is to sacrifice a thread for asynchronous MPI progression. However, neither do all MPI implementations support dedicated progression threads, nor did we succeed to use them robustly on our test system, nor are we eager to sacrifice a whole thread. Even if it is pinned to a hyperthread, a progression thread tends to pollute the runtime characteristics and caches.

We implemented a `progress` task (similar to [7]) which uses `MPI_Testsome` on the request manager’s request queue to make progress on outstanding MPI requests. In line with the polling, the task is started prior to the first time step and reschedules itself. Its rescheduling policy is different to the polling: Requeuing at the end of the ready queue turns out to be insufficient when a critical rank sends away tasks aggressively to victim ranks. A critical rank is per definition overloaded, i.e., has a long task queue. Too little investments into MPI progress yield late receives on the victim side. The progression task therefore forks an additional very high priority task if there are outstanding send requests. This task is terminated once no more outstanding send requests are remaining. On the receiving side, i.e., on an optimal victim rank, a very high

priority progression task is spawned if there are outstanding receive requests. The latter is terminated once the receiver’s set of active senders is empty.

Data calibration

Our reactive load balancing relies on online performance measurements which are distributed by non-blocking collective communication (`MPI_Iallgather`). With real time stamps, it is clear that an effective zero wait time does not manifest in a zero time span. We thus determine a threshold $t_{\min} = 0.95 \cdot \min_{i,j} t_{i,j}^{(\text{wait})} + 0.05 \cdot \max_{i,j} t_{i,j}^{(\text{wait})}$ for each rank, and drop all times below t_{\min} .

Nevertheless, some data remain biased: The wait time as defined in (1) notably suffers from snapshotting effects in MPI. Before we bookmark $N_i^{(\text{tasks})}(t)$, we run an additional instance of our polling task. It otherwise might happen that (1) assumes that no tasks were there even though they roam in MPI. This would eventually yield wrong timings and input into our algorithm.

We finally point out that (1) is a very idealised machine model: Our formula does anticipate that pending tasks can be done while we wait for incoming MPI messages and cores thus do not idle, but the formula does not distinguish where these remaining ready tasks come from. If no tasks are stolen, it is reasonable to assume a fixed cost $t^{(\text{task})}$ for a homogeneous set of pending tasks. If some of these tasks however are stolen tasks, their cost is higher, as we eventually have to send these tasks back. The vanilla version of (1) underestimates the local load, thus yields too high wait times, and eventually traps the reactive load balancing in an overbooking of victim ranks. It is therefore reasonable to reduce the local load further by a penalty which correlates linearly to the number of received tasks (which is encoded in our request manager).

7 Results

We benchmark our code on SuperMUC phase 2 and SuperMUC-NG at the Leibniz Supercomputing Centre (LRZ). Each of phase 2’s two-socket nodes contains two 14-core Intel Xeon E5-2687 v3 (Haswell) CPUs. Throughout the experiments, they have been clocked at 2.3 GHz. Infiniband FDR14 connects the individual nodes with a non-blocking pruned 4:1 tree. SuperMUC-NG hosts 2×24 cores of the Intel Xeon 8174 (Skylake) generation, which are clocked at 2.3 GHz and are connected through Intel Omni-Path. All shared memory parallelization relies on Intel’s Threading Building Blocks (TBB) [29] while Intel’s C++ compiler translated all codes. We use the 2018 generation of both tools on SuperMUC phase 2 and the 2019 generation of both tools on SuperMUC-NG.

Benchmarking with the baseline code on SuperMUC phase 2 has revealed that we achieve a shared memory efficiency well above 93% on one socket (Table 1) for a regular grid, while the four core setup even yields an efficiency of 100%. Performance deteriorates once we exceed 14 cores (a more detailed study on single-node performance, with emphasis on memory performance and scalability restrictions, was presented in previous work [9]). We therefore typically

Table 1: Shared memory parallel efficiency of our baseline code on one node without any offloading. We start from a $25 \times 25 \times 25$ grid and then add additional levels of (static) AMR. We measured the baseline using 2 threads.

Threads	Regular grid	One AMR level
4	1.00	1.00
7	0.97	0.97
14	0.93	0.87
28	0.53	0.48

run multiple-of-two ranks per node. For adaptive grids, our efficiency is only slightly worse. On one socket, our task parallelisation exposes some freedom to move tasks around.

Task and wait graph characterisation

We kick off our work distribution experiments with a showcase to illustrate the algorithms’ behaviour. The setup uses a $25 \times 25 \times 25$ grid (leading to a problem size of 72 Mio degrees of freedom) on a single Haswell node hosting eight MPI ranks. The load decomposition with eight ranks has to be imbalanced. We make the code dump all task outsourcing and wait time information and use these data to extract the graphs underlying our algorithmic mindset.

The graphs (Fig. 2) reveal that there is an overbooked rank 1 which delays our main time stepping loop running on rank 0. As rank 0 has to wait for rank 1, it in turn throttles the remaining six ranks that wait for a kick-off of the next time step. Such knock-on effects explain that our wait graphs will always resemble tree or forest graphs. It is reasonable to address the tails of the wait graphs to bring down the runtime iteratively.

The diffusive scheme, here ran with fixed $\omega^{(\text{diff})} = 1$, starts to gradually outsource tasks from the overbooked rank to all other ranks. The optimal victim role is passed on from one rank to the other (compare Fig. 2a and 2b) until all possible victims have been selected. The load distribution then stabilizes and is subsequently only altered by a small number of tasks. CCP yields a very similar task distribution scheme for the present setup. Our reactive diffusion thus is consistent in a numerical sense. Overall, CCP seems to balance more evenly across the ranks 2–7, while the number of offloaded tasks per rank is lower.

The task graphs’ black labels lead to a further interesting observation. Both balancing schemes derive a maximum number of tasks $N^{(\text{opt})}$ per rank which determines how many of these tasks can be given away. As tasks however first have to be created—an effect that amplifies for AMR where the task graph is unknown prior to the time step and dynamic refinement and coarsening can delay the creation of some tasks as the grid first has to be adopted—not all ranks fully exploit their task quota.

We continue to investigate this effect in further experiments where we use 16 MPI ranks distributed to 16 nodes and parametrise the number of cores available

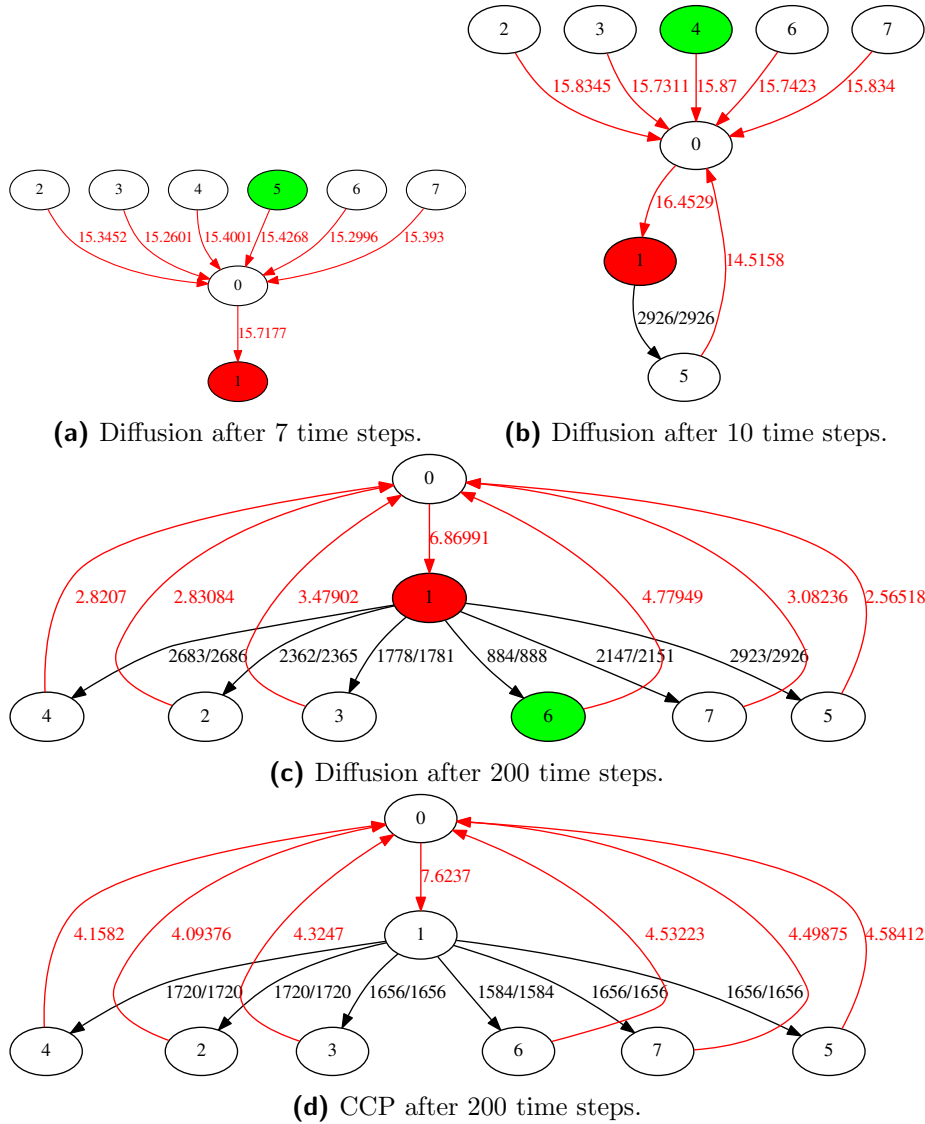


Figure 2: Wait and task distribution for the diffusive algorithm ((a)-(c)) and our task offloading using only the static CCP guess ((d)) for eight ranks. The critical rank is highlighted in red, the optimal victim in green. Red edges are wait times in seconds, black edges illustrate task offloading. The two given task numbers denote offloaded tasks vs. maximum tasks a rank would have been allowed to offload.

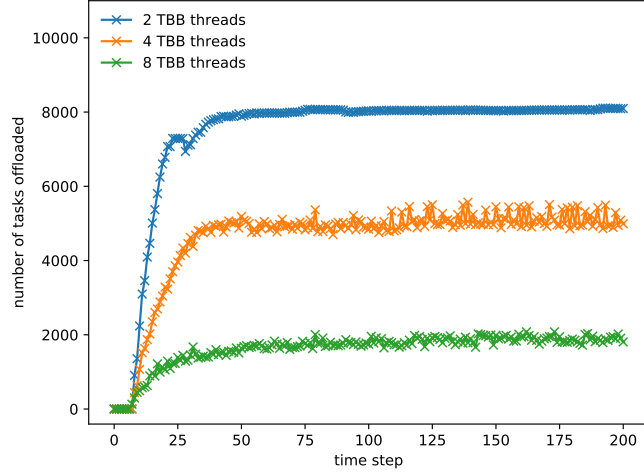


Figure 3: Run with 16 ranks (one MPI rank per node) where we vary the number of threads available to each rank.

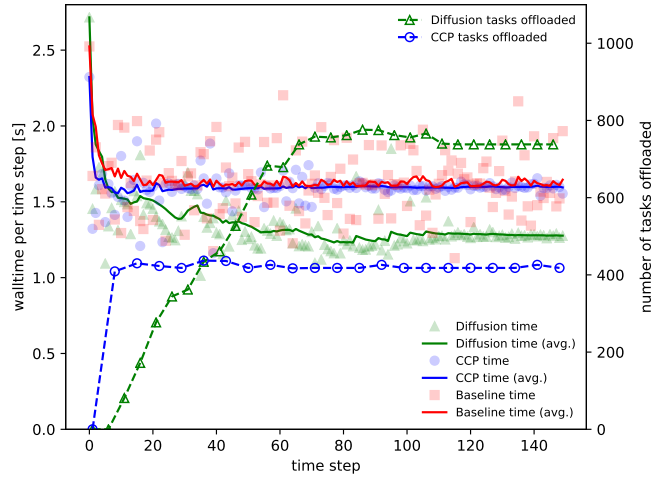


Figure 4: Comparison of CCP and diffusion with $\omega^{(\text{diff})} = 0.5$ to the baseline runtime. Per test, we present both the number of tasks that are offloaded and the runtime as gliding average as phrased by (2) (SuperMUC phase 2).

to each rank. We see ranks deploying the fewer tasks the more cores they have locally available (Fig. 3). For many codes deployed to multi-socket systems, it is reasonable to use more than one rank per node. This reduces NUMA effects[9]. Our reactive load balancing supports such a strategy. Otherwise, too many local cores have to be kept busy. These two technical advocates for multiple ranks per node finally are supported by the observation that more ranks give the domain decomposition more degrees of freedom how to distribute the mesh.

Comparison of baseline algorithms for an almost balanced mesh

We continue with a comparison of our two lightweight redistribution algorithms, CCP and reactive diffusion, to the baseline code performance. Again, the grid is fixed to $25 \times 25 \times 25$. We employ 28 ranks in total. Due to the dominance of the \mathcal{P} tasks, it is reasonable to assess the balancing quality in terms of the distribution of the space-time predictors: The lightest eight ranks host 512 of these tasks, while the heaviest rank hosts 729 \mathcal{P} s.

The measurements reveal (Fig. 4) how hard it is to balance and tune our baseline code—a property we consider to be prototypical for modern, task-based simulation codes: The runtimes per time step scatter significantly even though this is a regular grid setup without AMR. Closer inspection uncovers that the runtime does not randomly fluctuate but exhibits an oscillation-type pattern. Our code yields a task graph where individual tasks are optimistic. It is thus possible to bring tasks forward and to compute them in the (logically) previous iteration already. This leads to oscillating behaviour: One iterate finishes quickly. Tasks of the follow-up time step are set ready but not processed before the iteration reports “done” to the other ranks and completes its boundary data exchange. The subsequent iterate now has to process all of its tasks. At the same time, its task processing already spawns tasks of the subsequent iteration. Some of them are processed straight away as they sit in the ready queue. Compared to the previous time step, the present time step thus lasts longer. The fact that it already computes (some of) the tasks of the next iteration in turn makes the subsequent iterate finish fast again. We end up with oscillations.

Both of our balancing techniques reduce the oscillations. While it reduces the noise/scattering, CCP yields a time-averaged time per step which is hardly better than the runtime of the baseline code. CCP’s quasi-static “re”-balancing or “on-top”-balancing fails to improve the performance. The reason is that CCP is agnostic of the real time behaviour of the multithreaded code. A positive insight is that the offloading’s overhead is small, as we do not lose performance with CCP. CCP is not slower than the baseline.

The diffusive approach clearly outperforms CCP. It reduces the runtime almost monotonically and, once converged, brings the runtime per time step down from approximately 1.6s per step to around 1.2s.

The measurements support our decision to use work with (4) for measurements, and we observe that the diffusion, anticipating real hardware behaviour, calls for convergence acceleration techniques. The improvement of the runtime

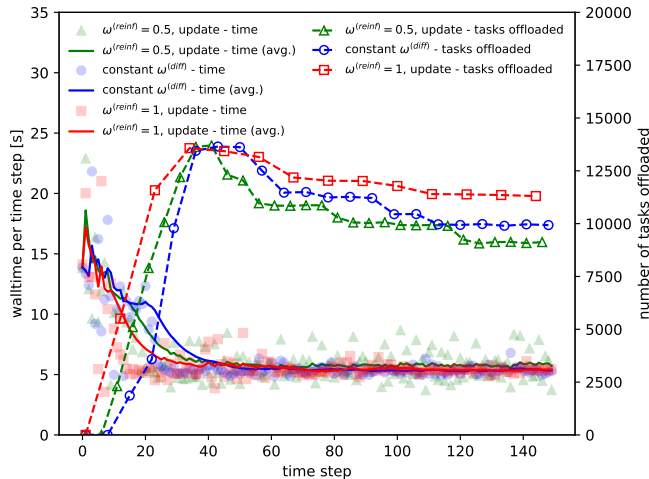


Figure 5: Runtime comparison of three executions of the diffusive algorithm. All executions start with $\omega^{(\text{diff})} = 1$. Two of them alter this diffusion parameter according to (3). We use a regular grid with $25 \times 25 \times 25$ cells on a single node hosting 14 ranks (SuperMUC phase 2).

is slow. Most importantly, the diffusion is faster than the static-cost model of CCP. Taking real measurements into account is important.

Convergence acceleration

Our work proposes to accelerate the damping update in (3) through a reinforcement technique. For all diffusion-based approaches, i.e. for any choice of $\omega^{(\text{diff})}$ and with and without an adaption of this value according to (3), the runtimes per time step eventually converge towards a similar value. Measurements in Fig. 5 show that our reactive approach tends to “over-balance”, unless we reduce $\omega^{(\text{diff})}$ in each time step. Over-balancing manifests in a large number of over offloaded tasks which trigger an emergency and thus induce a steep decline of tasks afterwards. It is only $\omega^{(\text{reinf})} = 1$, where no emergency is triggered and we thus do not observe a rapid decrease of offloaded tasks. With $\omega^{(\text{reinf})} = 1$, both overshooting and retreat are damped, as (3) triggers an almost monotonous decay of $\omega^{(\text{diff})}$. For $\omega^{(\text{reinf})} = 0.5$, the diffusion parameter is not immediately decreased. It even increases over the first few steps. And once a rank hits the blacklist, (3) increases $\omega^{(\text{diff})}$ of the rank which caused the blacklisting again. The rank consequently retreats quickly.

Both choices of a dynamic change of $\omega^{(\text{diff})}$ outperform a static diffusion constant. By means of a rapid reduction of runtime, a quick reduction of $\omega^{(\text{diff})}$ is the best choice after a massive rebalancing step which is induced here by the initial domain decomposition but also might result from dynamic AMR. We however do observe that quick re-increases of $\omega^{(\text{diff})}$ due to small $\omega^{(\text{reinf})}$ might

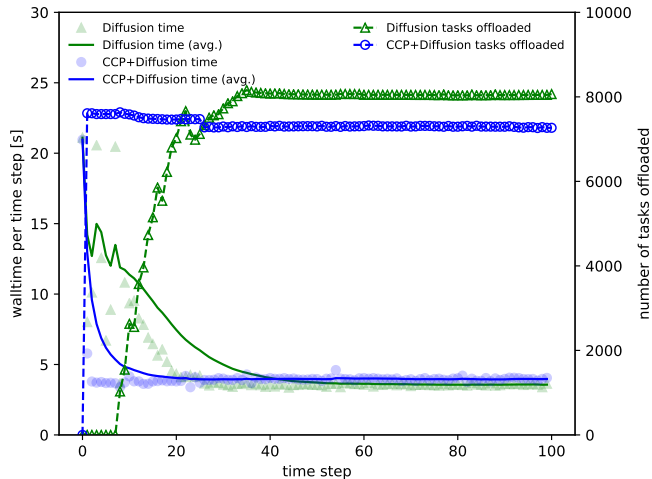


Figure 6: Runtime comparison of the diffusive algorithm with and without using CCP as an initial guess. We always initialise $\omega^{(\text{diff})} = 0.5$ (regular grid with $25 \times 25 \times 25$ cells on a single node of SuperMUC phase 2 hosting 14 ranks).

be reasonable if a small number of redistributed tasks is an objective, too. The reinforcement acts as additional penalty to the underlying optimisation problem which takes task offloading cost into account.

If we repeat our benchmark with 14 ranks ($\omega^{(\text{diff})} = 0.5$ and $\omega^{(\text{reinf})} = 1$), and benchmark our reactive scheme against CCP, we see CCP yield an aggressive initial task decomposition (Fig. 6). This is qualitatively in line with Fig. 4: CCP’s time per timestep is reduced much faster compared to the diffusion-only run. Reactive diffusion however is superior to CCP in the end as it takes the real behaviour of the machine into account. We emphasize that these experiments use CCP to determine the initial distribution but then let diffusion take over. CCP speeds up the initial distribution, but it also seems to steer the reactive approach into a local minimum, and diffusion fails then to improve upon this load balancing further.

Scaling studies

We continue our evaluation with some scaling studies. For this, we start with SuperMUC phase 2 and use the runtime per time step per degree of freedom on a single node as baseline. We normalise against the 28-core single node speed. Our data span 200 time steps, but we distinguish the runtimes within the first 50 iterations from the measurements within the remaining 150 steps. All following setups employ $\omega^{(\text{diff})} = 1$ and $\omega^{(\text{reinf})} = 1$.

Our first set of experiments (Table 2) study solely setups where we ensure that the geometric load balancing for the regular grid baseline is close to perfect. The baseline scaling thus is good, too. While the reactive diffusion improves

Table 2: Strong scaling speedups for a $25 \times 25 \times 25$ baseline grid. We separate time steps 1–25 (top) from 26–200 (bottom). AMR means that we add one level of AMR to the base grid. The reactive load balancing (LB) columns show by which factor the baseline scalability is improved. Entries smaller than 1 denote a slow-down, higher is better.

Nodes	Baseline scaling	reactive LB	
		regular grid	AMR
2	1.92	1.14	1.24
4	3.63	1.10	1.33
7	9.65	0.90	1.05
14	12.08	0.92	0.90
2	2.37	0.98	2.21
4	3.62	1.19	1.80
7	9.39	0.90	1.07
14	12.46	0.85	0.88

Table 3: Some typical reactive diffusion timings for various numbers of ranks. The mean runtime per time step for 200 time steps is given. The label “dyn” stands for dynamic AMR whereas “stat” denotes static AMR. We use a single refinement level for both variants of AMR. For dynamic AMR, the number of tasks $\#\mathcal{P}$ is changing over time.

Ranks	Nodes	$\#\mathcal{P}$	AMR	Base [t]=s	Diffusion [t]=s
4	1	-	dyn	18.0	14.4
7	1	-	dyn	15.3	12.7
40	20	33,201	stat	11.2	5.1
140	20	33,201	stat	8.1	4.6
280	20	33,201	stat	5.7	3.6

upon the regular grid runtimes for the smaller node choices, its contribution is limited through the strong scaling regime: If the nodes’ workload decreases, we eventually have enough cores available: It is cheaper to process tasks locally rather than to give them away—a decision encoded into our starvation check in Alg. 2.

With AMR, reactive load balancing robustly improves the walltime for these experiments with limited node counts (Table 3). A major selling point of AMR is its capability to allow codes to scale up problem sizes in a fine granular way, while work is invested where it pays off most. Equidistant global refinement in contrast would make the degrees of freedom and, hence, the memory footprint explode. As load balancing for varying grids is challenging, it is here where our approach helps most. It leverages the pressure to re-balance all the time and can compensate for slight ill-balancing.

We next benchmark our code systematically on multiple nodes of SuperMUC-NG on up to 731 ranks (Fig. 7). Two regular grids of $25 \times 25 \times 25$ or

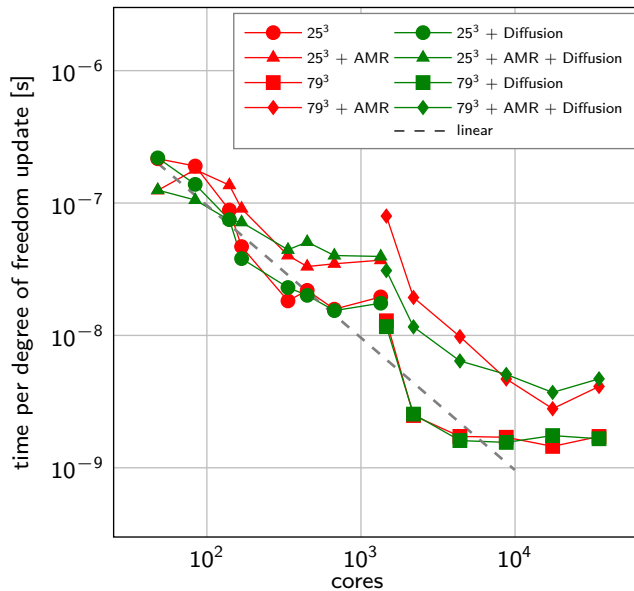


Figure 7: Strong scaling plots for various problem sizes with and without AMR on up to 731 ranks (SuperMUC-NG).

$79 \times 79 \times 79$ serve as starting point. We validated that the chosen geometric load balancing approach balances the regular grid setups almost perfectly. Indeed, we observe reasonable strong scaling behaviour for these regular grid configurations, i.e. runtimes decrease close to linearly with increasing core counts before they enter a stagnation regime. Our reactive load balancing does not make a real difference for these reasonably balanced setups. The important observation is, however, that it also does not impose any significant runtime penalty. This is due to its totally non-blocking implementation.

We finally allow our adaptivity criterion to add further cells to the regular base grids. For 25^3 and 79^3 this yields around $39 \cdot 10^6$ or $833 \cdot 10^6$ degrees of freedom, respectively. The baseline balancing here struggles to yield perfect decompositions. Indeed, we observe that the performance curves suffer from some offset, while the increased number of degrees of freedom, compared to the regular baseline grid, ensures that we scale to slightly more cores. Our reactive load balancing manages to narrow this gap between cost per degree of freedom in a perfectly balanced world vs. a world where we have to pay for the adaptivity and the resulting illbalancing. However, at large node counts, we run into the aforementioned issues (compare Fig. 3), where the task offloading is limited in the number of tasks that it can offload due to possible starvation of local cores. Indeed, some offloading-related overhead becomes visible.

8 Discussion

We introduce a very lightweight task migration pattern—lightweight in a sense that the baseline implementation is hardly changed—which allows us to use time otherwise spent in MPI waits for actual work. Many task systems already can exploit MPI waits to process (local) tasks, and our demonstrator realises this feature, too. However, we hypothesise that—in almost all cases—such an eager processing of ready tasks introduces idle time later down the line. It is thus reasonable to lighweightly “fill up” wait time with remote tasks from ranks that are overbooked. As our scheme migrates tasks non-persistently, this feature is particularly appealing for machines that suffer from speed fluctuations and for simulations where the load balancing is constrained due to the main memory available or load balancing overheads.

There are natural shortcomings of the present approach. First, our algorithms focus on ready tasks only. Tasks that have dependencies [6, 31] are not supported. On the long term, it is interesting to migrate whole task assemblies if a task set as a whole requires less data per computation to exchange than its individual tasks. Second, our algorithms are not yet memory aware. There is no quota on the maximum number of stolen tasks hosted by a victim. Victims consequently might exceed their memory. Memory consumption could be another blacklisting criterion. Third, we have chosen several “magic” parameters for our experiments. While they yield meaningful results, we can not claim that they are optimal. Autotuning here might improve the code’s performance. [16] Finally, it might be reasonable to take the network topology as well as the logical rank topology into account when a rank selects its victim. Rather than choosing the most underbooked rank globally, we could offload tasks to nearby ranks. This constrains the task migration but avoids that offloading adds more edges to the logical MPI communication graph that many codes tailor towards a network architecture.

The weakest point we see in terms of methodology is the lack of an appropriate notion of criticalness. Our experiments run into situations where victim ranks are given too many remote tasks. This delays their actual delivery of information such as boundary data and eventually slows down critical ranks further. They however do not recognise this as they are not waiting for an outsourced task. Such complex causal dependencies can not be tracked by our current notion of an emergency. We track overloading in a compute sense, but lack a detector for overloading in a bandwidth or MPI overhead (too many pending non-blocking messages) sense.

We have extensively invested into a scheme which ensures that reasonable progress is made on the asynchronous MPI transfers without sacrificing a thread [18]. We use aggressive polling. Yet, this cannot detect congestion. While the prioritisation of MPI messages might mitigate this problem to some degree, we would appreciate if there were an MPI monitoring, i.e., online performance analysis that can tell the application if the MPI subsystem enters a critical state. This could be realised via software [23] supervising the machine state. Alternatively, “intelligent” communication devices alike the SmartNIC technology

could host the monitoring.

On the shared memory side, it remains open to which degree our choice of TBB as tasking base with manual tweaking of features like prioritisation affects the performance results. All proposed software building blocks currently are extracted into a standalone software package such that they can be used more easily with other codes [22]. As part of this roll out, we also explore the integration into OpenMP. On the long term an abstraction over various tasking paradigms [3] however might become necessary, such that we can systematically study the interplay of tasking approach and our balancing.

Our lightweight task migration realises push semantics: Oversubscribed ranks deploy work to other ranks. This approach differs to strategies where ranks know their task workload prior to the computation—though they might permanently renegotiate, i.e. balance such responsibilities—or codes with pull semantics, where ranks “grab” tasks from a (distributed) repository [25]. While all paradigms might yield comparable data distribution graphs, our code migrates tasks only temporarily, i.e. sends results back. Our induced data flow graph is cyclic. It is thus lightweight as it does not redistribute data permanently. It is not lightweight by means of data moves, as every temporary task migration relies on a send forth and a send back.

9 Outlook

The exact interplay of our scheme with various dynamic load balancing schemes or more sophisticated numerics is beyond scope for the present paper. We do however expect that our approach has beneficial knock-on effects: If load balancing is semi-static [6], i.e., rebalanced only every k steps, we may assume that our approach allows us to migrate work less frequently (similar to [30]). This reduces AMR overhead. If load is balanced continuously in a diffusive style, we may assume that the diffusion rate, i.e., the amount of data migration per step, can be chosen smaller with our approach. This reduces bandwidth requirements. On accelerator-driven machines, where bandwidth and local memory are notoriously short, we may assume that our approach offers an alternative to the difficult heterogeneous scheduling [32]. Our approach would make each accelerator a designated victim and thus hide the complexity of persistent data migration to balance load between accelerators.

On the numerics side, we will investigate non-linear equation systems in the ADER-DG context. Such schemes require iterative Picard or Newton solves per \mathcal{P} task [36]. This renders the cost per \mathcal{P} evaluation very hard to predict. ADER-DG is often contrasted with standard Runge-Kutta (RK) methods. Indeed, our ideas should apply to RK as well, though their lack of a space-time evaluation might imply that the evolution of the cells is cheaper. In return, we might get away with a smaller memory footprint. This renders RK another interesting numerical scheme to study. ADER-DG’s attractiveness is its inherent fit to adaptive, local time stepping. Again, such a time stepping renders the workload prediction very difficult. It thus should benefit from our approach. Fi-

nally, we plan, on the long term, to study the interplay of our Eulerian mindset with Lagrangian techniques (see [14] or [35], the latter also working on tree-structured adaptive Cartesian grids). While the load inhomogeneity resulting from these couplings is obvious, it is notably the fact that such setups have to balance both memory and compute load rigorously which makes it interesting for our approach.

Acknowledgements

This work has received funding from the European Union’s Horizon 2020 research and innovation programme under grant agreement No 671698 (ExaHyPE). We also acknowledge support and computing resources provided by the Leibniz Supecomputing Centre (grant no pr48ma). Special thanks are due to all members of the ExaHyPE consortium who made this research possible – in particular to Leonhard Rannabauer for his work on the elastic wave equation solver and the LOH.1 setup. All underlying software is open source [4].

References

- [1] B. Acun, A. Gupta, N. Jain, A. Langer, H. Menon, E. Mikida, X. Ni, M. Robson, Y. Sun, E. Totonì, L. Wesolowski, and L. Kale. Parallel programming with migratable objects: Charm++ in practice. In *Proceedings of the International Conference for High Performance Computing, Networking, Storage and Analysis, SC ’14*, pages 647–658. IEEE Press, 2014.
- [2] B. Acun, P. Miller, and L. V. Kale. Variation among processors under turbo boost in hpc systems. In *Proceedings of the 2016 International Conference on Supercomputing, ICS ’16*, pages 6:1–6:12, New York, NY, USA, 2016. ACM.
- [3] R. Alomairy, H. Ltaief, M. Abduljabbar, and D. Keyes. Abstraction layer for standardizing apis of task-based engines. Technical report, King Abdullah University of Science and Technology, 2019. <http://hdl.handle.net/10754/656693>.
- [4] M. Bader, M. Dumbser, A.A. Gabriel, H. Igel, L. Rezzolla, and T. Weinzierl. ExaHyPE—an Exascale Hyperbolic PDE solver Engine, 2019. <http://www.exahype.eu>.
- [5] L. Bottou, F. Curtis, and J. Nocedal. Optimization methods for large-scale machine learning. *SIAM Review*, 60(2):223–311, 2018.
- [6] M. H. Bremer, J. D. Bachan, and C. P. Chan. Semi-static and dynamic load balancing for asynchronous hurricane storm surge simulations. In SC18, editor, *2018 IEEE/ACM Parallel Applications Workshop, Alternatives To MPI, PAW-ATM@SC 2018, Dallas, TX, USA, November 16, 2018*, pages 44–56, 11 2018.

- [7] D. Buettner, J.-T. Acquaviva, and J. Weidendorfer. Real asynchronous MPI communication in hybrid codes through OpenMP communication tasks. In *Proceedings of the 2013 International Conference on Parallel and Distributed Systems*, ICPADS '13, pages 208–215, Washington, DC, USA, 2013. IEEE Computer Society.
- [8] J. Charles, P. Jassi, N. S. Ananth, A. Sadat, and A. Fedorova. Evaluation of the intel core i7 turbo boost feature. In *2009 IEEE International Symposium on Workload Characterization (IISWC)*, pages 188–197, Oct 2009.
- [9] D. E. Charrier, B. Hazelwood, E. Tutlyaeva, M. Bader, M. Dumbser, A. Kudryavtsev, A. Moskovsky, and T. Weinzierl. Studies on the energy and deep memory behaviour of a cache-oblivious, task-based hyperbolic pde solver. *The International Journal of High Performance Computing Applications*, 33(5), 2019. arXiv:1810.03940.
- [10] D. E. Charrier, B. Hazelwood, and T. Weinzierl. Enclave tasking for discontinuous galerkin methods on dynamically adaptive meshes. 2019. arXiv:1806.07984 (submitted).
- [11] D. E. Charrier and T. Weinzierl. Stop talking to me—a communication-avoiding ader-dg realisation. 2019. arXiv:1801.08682 (submitted).
- [12] J. Davison de St. Germain, J. McCorquodale, S. G. Parker, and C. R. Johnson. Uintah: a massively parallel problem solving environment. *The Ninth International Symposium on High-Performance Distributed Computing*, pages 33–41, 2000.
- [13] S. M. Day, J. Bielak, D. Dreger, S. Larsen, R. Graves, A. Pitarka, and K. B. Olsen. Tests of 3d elastodynamics codes: Final report for lifelines program task 1a02. Technical report, 2003.
- [14] A. Dubey, K. Antypas, and C. Daley. Parallel algorithms for moving Lagrangian data on block structured Eulerian meshes. *Parallel Computing*, 37(2):101 – 113, 2011.
- [15] M. Dumbser and M. Käser. An arbitrary high order discontinuous Galerkin method for elastic waves on unstructured meshes ii: The three-dimensional isotropic case. *Geophysical Journal International*, 167(1):319–336, 2006.
- [16] W. Eckhardt, R. Glas, D. Korzh, S. Wallner, and T. Weinzierl. On-the-fly memory compression for multibody algorithms. In G. R. Joubert, H. Leather, M. Parsons, F. Peters, and M. Sawyer, editors, *Adv. in Parallel Comput.*, volume 27, pages 421–430, 2015.
- [17] J. S. Hesthaven and T. Warburton. *Nodal Discontinuous Galerkin Methods: Algorithms, Analysis, and Applications*, volume Texts in Applied Mathematics 54. Springer, 2008.

- [18] T. Hoefer and A. Lumsdaine. Message progression in parallel computing—to thread or not to thread? In Y. Ishikawa, editor, *2008 IEEE International Conference on Cluster Computing*, pages 213–222, 2008.
- [19] H. Igel. *Computational Seismology: A Practical Introduction*. Oxford University Press, 1. edition, 2016.
- [20] N. Jain, A. Bhatele, L. H. Howell, D. Böhme, I. Karlin, E. A. León, M. Mubarak, N. Wolfe, T. Gamblin, and M. L. Leininger. Predicting the performance impact of different fat-tree configurations. In *Proceedings of the International Conference for High Performance Computing, Networking, Storage and Analysis, SC '17*, pages 50:1–50:13, New York, NY, USA, 2017. ACM.
- [21] H. Kaiser, T. Heller, B. Adelstein-Lelbach, A. Serio, and D. Fey. Hpx: A task based programming model in a global address space. In *Proceedings of the 8th International Conference on Partitioned Global Address Space Programming Models, PGAS '14*, pages 6:1–6:11, New York, NY, USA, 2014. ACM.
- [22] J. Klinkenberg, P. Samfass, M. Bader, and C. Terboven. Reactive task migration for hybrid mpi+openmp applications. PPAM 2019, Bialystok, Poland, accepted, 2019.
- [23] G. Mao, D. Böhme, M.-A. Hermanns, M. Geimer, D. Lorenz, and F. Wolf. Catching idlers with ease: A lightweight wait-state profiler for mpi programs. pages 103:103–103:108, 09 2014.
- [24] J. D. McCalpin. HPL and DGEMM performance variability on the Xeon Platinum 8160 processor. In *Proceedings of the International Conference for High Performance Computing, Networking, Storage, and Analysis, SC '18*, pages 18:1–18:13, Piscataway, NJ, USA, 2018. IEEE Press.
- [25] Q. Meng, J. Luitjens, and M. Berzins. Dynamic task scheduling for the uintah framework. In I. Raicu, I. Foster, and Y. Zhao, editors, *2010 3rd Workshop on Many-Task Computing on Grids and Supercomputers*, pages 1–10, 2010.
- [26] A. Pinar and C. Aykanat. Fast optimal load balancing algorithms for 1d partitioning. *Journal of Parallel and Distributed Computing*, 64(8):974–996, 2004.
- [27] S. D. Pollard, N. Jain, S. Herbein, and A. Bhatele. Evaluation of an interference-free node allocation policy on fat-tree clusters. In *Proceedings of the International Conference for High Performance Computing, Networking, Storage, and Analysis, SC '18*, pages 26:1–26:13, Piscataway, NJ, USA, 2018. IEEE Press.

- [28] A. Reinarz, M. Bader, L. Bovard, D. Charrier, M. Dumbser, K. Duru, F. Fambri, A. Gabriel, JM Gallard, S. Köppel, L. Rannabauer, L. Rezzolla, P. Samfaß, M. Tavelli, and T. Weinzierl. ExaHyPE: an engine for parallel dynamically adaptive simulations of wave problems. *Submitted to Computational Physics Communications*, 2019.
- [29] J. Reinders. *Intel Threading Building Blocks*. O'Reilly & Associates, Inc., first edition, 2007.
- [30] P. Samfass, J. Klinkenberg, and M. Bader. Hybrid mpi+openmp reactive work stealing in distributed memory in the pde framework sam(oa)². In D. S. Nikolopoulos and B. R. de Supinsk, editors, *2018 IEEE International Conference on Cluster Computing (CLUSTER)*, pages 337–347, 2018.
- [31] M. Schaller, P. Gonnet, A. B. G. Chalk, and P. W. Draper. SWIFT: using task-based parallelism, fully asynchronous communication, and graph partition-based domain decomposition for strong scaling on more than 100,000 cores. In *Proceedings of the Platform for Advanced Scientific Computing Conference, PASC '16*, pages 2:1–2:10, New York, NY, USA, 2016. ACM.
- [32] H. Sundar and O. Ghattas. A nested partitioning algorithm for adaptive meshes on heterogeneous clusters. In ICS '15, editor, *Proceedings of the 29th ACM on International Conference on Supercomputing*, pages 319–328, 2015.
- [33] The Stellar Group. Hpx, 2019. <http://stellar-group.org/tag/hpx>.
- [34] T. Weinzierl. The Peano software – parallel, automaton-based, dynamically adaptive grid traversals. *ACM Transactions on Mathematical Software (TOMS)*, 45(2):14:1–14:41, 2019.
- [35] T. Weinzierl, B. Verleye, P. Henri, and D. Roose. Two particle in tree realisations. *Parallel Computing*, 52:42–64, 2016.
- [36] O. Zanotti, F. Fambri, M. Dumbser, and A. Hidalgo. Space-time adaptive ader discontinuous galerkin finite element schemes with a posteriori sub-cell finite volume limiting. *Computers & Fluids*, 118:204–224, 2015.